Stabilization of Helical Macromolecular Phases by Confined Bending

Matthew J. Williams[1,*] and Michael Bachmann[1,2,3,†]

[1]Soft Matter Systems Research Group, Center for Simulational Physics, The University of Georgia, Athens, Georgia 30602, USA
[2]Instituto de Física, Universidade Federal de Mato Grosso, 78060-900 Cuiabá (MT), Brazil
[3]Departamento de Física, Universidade Federal de Minas Gerais, 31270-901 Belo Horizonte (MG), Brazil

(Received 18 March 2015; revised manuscript received 11 June 2015; published 21 July 2015)

By means of extensive replica-exchange simulations of generic coarse-grained models for helical polymers, we systematically investigate the structural transitions into all possible helical phases for flexible and semiflexible elastic polymers with self-interaction under the influence of torsion barriers. The competing interactions lead to a variety of conformational phases including disordered helical arrangements, single helices, and ordered, tertiary helix bundles. Most remarkably, we find that a bending restraint entails a clear separation and stabilization of the helical phases. This aids in understanding why semiflexible polymers such as double-stranded DNA tend to form pronounced helical structures and proteins often exhibit an abundance of helical structures, such as helix bundles, within their tertiary structure.

DOI: 10.1103/PhysRevLett.115.048301 PACS numbers: 82.35.Lr, 64.70.-p, 83.10.Tv, 87.15.Cc

Helical segments are ubiquitous secondary structures occurring in most macromolecular systems. The emergence of helical structures is typically attributed to the formation of hydrogen bonds along the backbone of linear polymers, but it is also known that helices are among the few generic geometries that a linelike topology can form if an ordering principle (such as a many-body constraint) is present [1–3].

In seminal works, Zimm and Bragg (ZB) [4,5] showed that the crossover between disordered random coil structures and ordered helical conformations can be described by a one-dimensional Ising-like model. Therefore, while short-range cooperativity can lead to structural ordering, in the ZB model, this process is not a phase transition in the strict thermodynamic sense [6,7]. However, since biologically relevant macromolecules are finite systems (on an effectively mesoscopic scale), the thermodynamic interpretation of structural transitions in such systems must address finiteness effects accordingly [8].

Primary effects of cooperativity can be addressed by generic effective-potential models that allow for the qualitative description of helix-coil transitions [9–12]. Dominant nonbonded interactions support the formation of tertiary structures including single helices, helix bundles, collapsed globules, or random coils [13–20]. It has been shown recently that the alignment of secondary structures in a tertiary protein fold can be understood as a simple two-state process [21].

For a generic flexible polymer chain, in a crystallization process succeeding the chain collapse, ordered structures emerge that are substantially different from tertiary structures known from realistic biomolecules and typically do not possess secondary structures [22,23]. If bending restraints and nonbonded interaction compete with each other, as it is the case in self-interacting semiflexible polymers, the ordered structures are known to be rodlike bundles or toroids [24].

However, less is known about the influence of effective bending restraints upon transition pathways toward helical structures. A systematic analysis of the formation and separation of helical phases in phase space in the presence or absence of bending restraints has not yet been performed. In this study, we investigate the relevance of this restraint for the separation of structural phases by means of replica-exchange Monte Carlo computer simulations for coarse-grained flexible and semiflexible polymer models. By scanning the spaces of torsion parameter strength and temperature, we construct the hyperphase diagrams for entire classes of helical macromolecules, which allows us to distinguish the different pathways to the helical folds and enables us to judge the significance of bending restraints in biomacromolecules.

We employ a generic coarse-grained bead-spring model for elastic, self-interacting polymers with torsional interaction. The polymer is represented by a linear chain of N monomers. The bending energy of flexible polymers is zero. For semiflexible polymers, excitations of the bond angle formed by successive bonds are subject to an energetic penalty. Torsion is induced by an out-of-plane torsion angle between three successive bonds. Nonbonded monomers interact via long-range attractive and short-range repulsive van der Waals forces, modeled by the Lennard-Jones (LJ) potential. The energy of a conformation $\mathbf{X} = \{\mathbf{x}_1, \mathbf{x}_2, \ldots, \mathbf{x}_N\}$, where $\mathbf{x}_i$ is the location of the ith monomer, is given in units of the LJ energy scale ϵ by $E(\mathbf{X})/\epsilon = \sum_{i>j+1} v_{\mathrm{LJ}}(r_{ij}) + s_r \sum_i v_{\mathrm{bond}}(r_{ii+1}) + s_\theta \sum_k v_{\mathrm{bend}}(\theta_k) + s_\tau \sum_l v_{\mathrm{tor}}(\tau_l)$. The dimensionless Lennard-Jones potential with cutoff is given by $v_{\mathrm{LJ}}(r) = 4[(\sigma/r)^{12} - (\sigma/r)^6] - v_c$ if $r < r_c = 2.5\sigma$, where r is the distance between two nonbonded monomers and $v_c \approx -0.0163$ is a constant shift to ensure $v_{\mathrm{LJ}}(r_c) = 0$. For $r > r_c$, $v_{\mathrm{LJ}}(r) = 0$. Distances are measured in units of the

length scale r_0, given by the location of the LJ potential minimum. The van der Waals radius of a monomer is $\sigma = 2^{-1/6} r_0$. The finitely extensible nonlinear elastic (FENE) bond potential is employed in the form [25] $v_{\text{bond}}(r) = \log\{1 - [(r - r_0)/R]^2\}$. The bond strength is $s_r = -KR^2/2\epsilon$; the parameters were set to standard values $K = (98/5)\epsilon r_0^2$ and $R = (3/7) r_0$. The payoff for bending the chain is $v_{\text{bend}}(\theta) = 1 - \cos(\theta - \theta_0)$, where θ_0 is the bond angle in the ground state. The bending energy scales with $s_\theta = S_\theta/\epsilon$. For the simulations of the flexible polymer $S_\theta = 0$ (no bending restraint), whereas for the semiflexible polymer $S_\theta = 200\epsilon$ was chosen. Eventually, the torsion potential is $v_{\text{tor}}(\tau) = 1 - \cos(\tau - \tau_0)$, with the dihedral torsion angle τ and its equilibrium value τ_0. The relative energy scale is $s_\tau = S_\tau/\epsilon$. The choice of reference angles $\tau_0 = 0.873$ and $\theta_0 = 1.742$ allows for helical segments in the ground-state structures that resemble right-handed α helices with about four monomers per turn. In the following, ϵ, r_0, and k_B are set to unity. For the simulation of polymers with up to 60 monomers, replica-exchange Monte Carlo parallel tempering simulations were performed [26–29].

The propensities of polymers with ($S_\theta > 0$) and without bending restraint ($S_\theta = 0$) to form stable helical structures are investigated under thermal conditions controlled by the canonical heat-bath temperature T. The variation of the torsion strength S_τ enables the study of an entire class of helical polymers. Representations of transition channels in generalized ensembles have turned out to be beneficial [8,30–32]. Therefore, we discuss the folding channels of the helical polymers in the multiplicative canonical ensemble provided by the parallel tempering method. We introduce a pair of order parameters which are effectively defined by the average total energies per monomer of the nonbonded LJ interactions between all monomers and their neighbors up to six bonds away,

$$q_1(\mathbf{X}) = \epsilon \frac{1}{N} \sum_{i=1}^{N-2} \sum_{j=i+2}^{N} \Theta_{6,j-i} v_{\text{LJ}}(r_{ij}), \tag{1}$$

and all others,

$$q_2(\mathbf{X}) = \epsilon \frac{1}{N} \sum_{i=1}^{N-2} \sum_{j=i+2}^{N} \Theta_{j-i,7} v_{\text{LJ}}(r_{ij}), \tag{2}$$

where $\Theta_{kl} = 1$ if $k \geq l$ and zero otherwise. In a single long helix, q_1 is minimal and q_2 maximal, whereas for helix bundles with increasing number of segments q_2 gets smaller and q_1 larger.

For a 40-mer, Fig. 1 depicts for a selection of torsion strength values S_τ the distributions of conformations found in the generalized ensemble that covers the temperature interval $T \in [0.1, 2.0]\epsilon/k_B$ in (q_1, q_2) space. The left column of Fig. 1 shows the helical transition pathways for the bending-restrained semiflexible polymer ($S_\theta = 200\epsilon$) and the right column for the unrestrained flexible polymer ($S_\theta = 0$). The light gray region represents the area in (q_1, q_2) space, in which conformations were found at all temperatures and torsion strengths in the simulations. This distribution, which is independent of T and S_τ, gives a first impression of the differences of the conformational phases of entire classes of semiflexible and flexible polymers. It

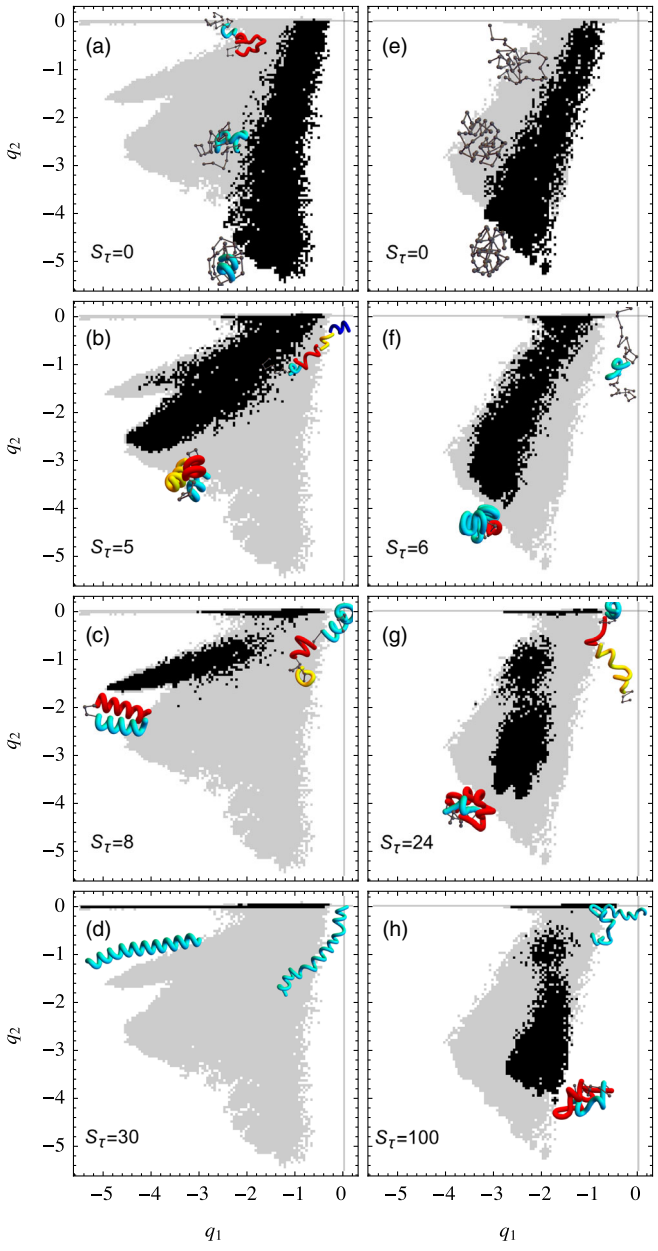

FIG. 1 (color online). Scatter plots of conformations of the (a)–(d) semiflexible (bending restrained) and (e)–(h) flexible (bending unrestrained) polymers with 40 monomers in (q_1, q_2) space. Light gray regions represent the generalized ensemble of all conformations found at all temperatures T and torsion strengths S_τ simulated. Black regions correspond to the most populated states at given S_τ values. Representative conformations are shown.

depicts the possible folding channels for the polymers. From the figure, it is obvious that the distributions spread out much more for the bending-restrained polymer. Individual sections (phases) are clearly separated, with less-populated regions in between. This is different in the case of flexible polymers. Although conformational phases can be identified as well, their separation is much less prominent. These differences can be interpreted in the way that in the case of semiflexible helical polymers, structural phases are more stable, because these are surrounded by entropically suppressed regions, which cause free-energy barriers and phase separation between the helical phases. The black regions in the figures represent the populations in (q_1, q_2) for fixed S_τ values, i.e., for individual polymer systems and confirm that semiflexible polymers with a certain torsion strength prefer to form tertiary structures inside a distinct helical phase only, which is not the case for flexible polymers.

The differences in their structural behavior are also clearly visible when plotting the order parameter ratio $\langle q_2\rangle/\langle q_1\rangle$ for the lowest-energy structures found in the simulations, as shown in Fig. 2. The steplike decrease of this ratio for the bending-restrained polymers enables the location of the threshold values of S_τ where structural phases are separated.

For a more systematic analysis of the folding behavior and its dependence on the torsion strength S_τ and temperature T, we define the free energy in order parameter space by $F_{S_\tau,T}(q_1, q_2) = -k_B T \log Z_{S_\tau,T}(q_1, q_2)$, where $Z_{S_\tau,T}(q_1', q_2') = \int \mathcal{D}X \delta(q_1' - q_1(\mathbf{X}))\delta(q_2' - q_2(\mathbf{X}))\times \exp[-E(\mathbf{X})/k_B T]$ is the restricted partition function in the space of all polymer conformations $\{\mathbf{X}\}$. Fixing S_τ and T, the free energy $F_{S_\tau,T}(q_1, q_2)$ possesses a global minimum at order parameter values $(q_1^{\min}, q_2^{\min})$. The ensemble of all conformations with these order parameter values represents a dominant macrostate of the system. The space of macrostates that share a characteristic structural feature such as the number of helical segments in a helix bundle forms a structural phase.

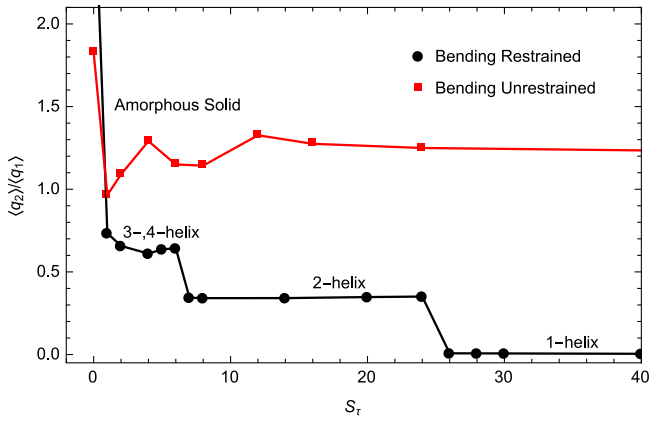

FIG. 2 (color online). Ratio of order parameters $\langle q_2\rangle/\langle q_1\rangle$ for lowest-energy structures at various values of S_τ in the cases of restrained and unrestrained bending.

Transitions temperatures for the various model parameter settings were identified by standard canonical analyses of extremal fluctuations of energy (specific heat), structural quantities (e.g., radius of gyration), and order parameters ($\langle q_1\rangle$, $\langle q_2\rangle$, number of helices). This will be discussed in more detail elsewhere [33]. Based on this information, the (q_1, q_2) space can be separated into regions ("structural phases") as shown in Fig. 3 for bending-restrained semiflexible (left figure) and unrestrained, flexible polymers (right figure). Black lines represent folding trajectories for several single polymers with fixed torsion strengths in the interval $S_\tau \in [0, 30]$ in (q_1, q_2) space upon cooling. All trajectories begin in the high-temperature, random-coil phase (upper right corner in Fig. 3, i.e., large q_1, q_2 values) and propagate toward a helical state by decreasing the temperature. The folding channels at given S_τ values effectively connect free-energy minima (dots) at various temperatures.

The structural phases of flexible polymers are less well separated, in which case folding channels, after passing a liquid phase, end in the solid amorphous phase. This general transition behavior is virtually independent of the torsion strength S_τ. However, the influence of the value of S_τ upon helix and helix-bundle formation is significant for the bending-restrained, semiflexible polymer. For $S_\tau = 0$, the behavior is similar to that of the flexible polymer, but for torsion strength $S_\tau = 1$, it crystallizes initially into a three-helix bundle and then undergoes a solid-solid transition. It emerges from it as a four-helix bundle, which is energetically slightly more favorable at very low temperatures. Three-helix bundles clearly form at sufficiently large torsion strength (e.g., for $S_\tau = 5$).

Increasing the torsion strength further favors the extension of helical segments, compared to local nonbonded contacts. The torsional interaction overcompensates what had been an energetic gain of nonbonded monomer-monomer contacts despite necessary bending penalties. The number of turns is reduced to a single one and a double-helix forms in the solid phase ($S_\tau = 8$). Bending-restrained polymers with $S_\tau = 20$ coexist in a transition state between a single and double-helix; i.e., in an intermediate ordered solid phase a single helix is formed first, which upon further cooling splits into a double-helix at the expense of the formation of a single turn. This torsion strength marks the threshold at which distant monomer-monomer contacts are still formed. For torsion strengths close to $S_\tau = 30$ and beyond, only stable single-helix phases form.

The complete structural hyperphase diagram, parametrized by temperature T and torsion strength S_τ, is depicted in Fig. 4 for bending-restrained, semiflexible polymers (left) and for unrestrained, flexible polymers with torsion (right). The phase diagram for the semiflexible polymer

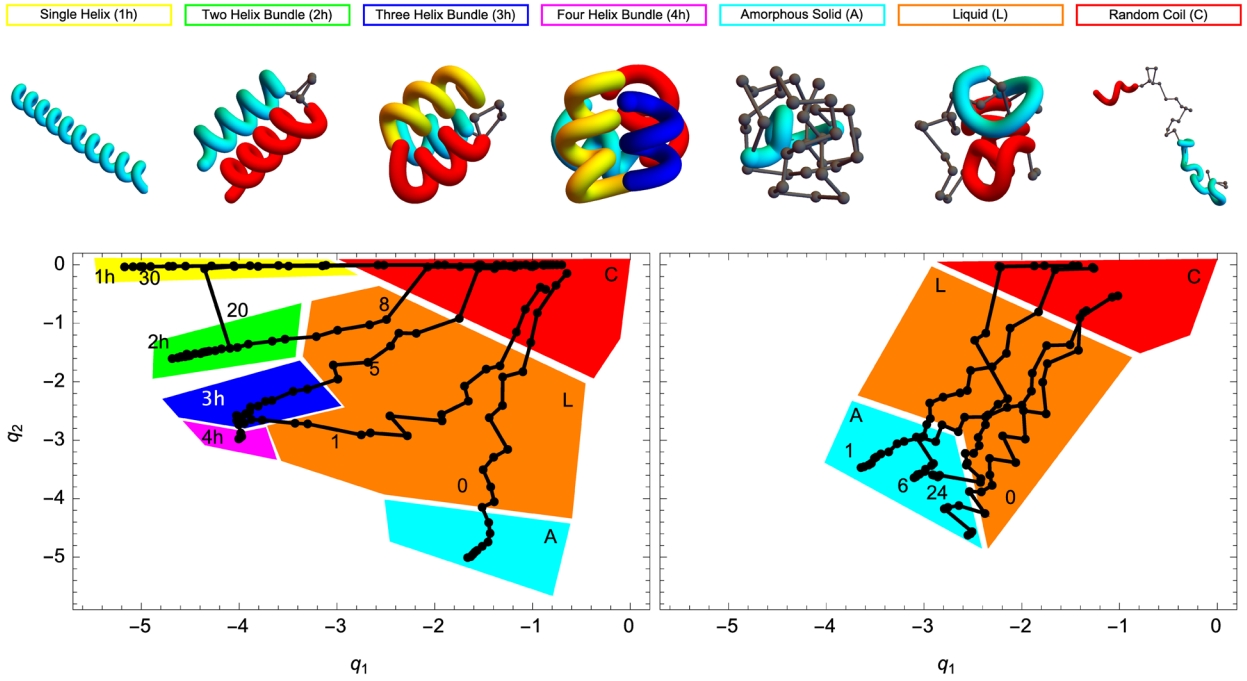

FIG. 3 (color online). Structural phase diagrams for bending-restrained semiflexible (left) and unrestrained flexible polymers (right) in (q_1, q_2) order parameter space for the temperature and torsion strength space (T, S_τ) covered in our simulations. Colored regions represent structural phases. Black dots locate free energy minima at given T and S_τ values. Trajectories show the helical folding pathways at fixed torsion strengths S_τ by decreasing the temperature.

exhibits apparently more structure in the folded regime at temperatures $T < 0.5$ over the entire interval of torsion strengths. Whereas at torsion strengths $S_\tau < 7$ four-helix bundles, three-helix bundles, and amorphous conformations compete and the phases sensitively depend on the temperature, two-helix bundles and single-helix conformations are clearly dominant for $S_\tau > 7$. Remarkably, the liquid (globular) phase disappears for sufficiently large torsion strengths ($S_\tau > 15$), in which case direct coil-helix transitions occur. Within the range $15 < S_\tau < 27$, helix-helix (solid-solid) transitions are present, where single helices collapse into two-helix bundles by forming a turn. Once the torsion strength dominates over nonbonded monomer-monomer interaction, i.e., for $S_\tau > 27$, the well-known direct transition from random coils into single helices occurs.

Contrarily, the folding process of flexible polymers is hardly affected qualitatively by torsional constraints [Fig. 4 (right)]. The three phases of random coils, globular, and amorphous structures are well separate, but a helical phase is nonexistent. Furthermore, if bending is *not* restrained, the liquid phase does not disappear and thus a helix-coil transition does not occur.

In this Letter, we have systematically investigated the influence of bending restraints upon the formation of stable helical phases. We determined all structural phases for entire classes of flexible and semiflexible polymers with torsion. These results were summarized in structural hyperphase diagrams for both polymer classes.

The primary result of our study is that an effective bending restraint along the polymer chain is necessary to stabilize helical structures and, in particular, helix bundles. Different helical structure types that are separated by entropic gaps in conformational space can only be identified clearly for semiflexible polymers, whereas for flexible polymers torsional barriers alone are not sufficient to stabilize individual helical phases.

The outcome of this study provides evidence for the natural preference and significance of locally ordered

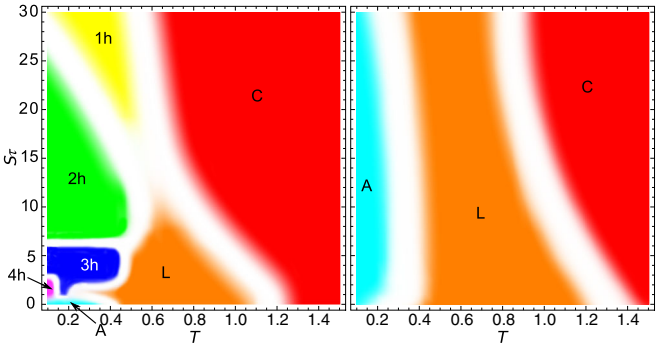

FIG. 4 (color online). Hyperphase diagrams of bending-restrained semiflexible (left) and unrestrained flexible polymers (right) with 40 monomers, represented in the space of the torsion strength S_τ as a material parameter distinguishing classes of polymers and the temperature T as an external control parameter for the formation of structural phases. The color code is the same as in Fig. 3.

helical secondary structures for semiflexible biopolymers, which effectively include DNA and most proteins. Our results support the understanding of the almost strict confinement of bond angles in polypeptides (such as bioproteins), which reduces the set of degrees of freedom that participate in their functional structure formation to dihedral angles. For this reason, it is unlikely that flexible polymers, i.e., polymers without bending restraint, can be vital and functional in a biological system.

This work has been supported partially by the NSF under Grant No. DMR-1207437 and by CNPq (National Council for Scientific and Technological Development, Brazil) under Grant No. 402091/2012-4.

*mjw532@uga.edu
†bachmann@smsyslab.org
http://www.smsyslab.org

[1] A. Maritan, C. Micheletti, A. Trovato, and J. R. Banavar, Nature (London) **406**, 287 (2000).
[2] T. Vogel, T. Neuhaus, M. Bachmann, and W. Janke, Europhys. Lett. **85**, 10003 (2009).
[3] T. Vogel, T. Neuhaus, M. Bachmann, and W. Janke, Phys. Rev. E **80**, 011802 (2009).
[4] B. Zimm and J. Bragg, J. Chem. Phys. **28**, 1246 (1958).
[5] B. Zimm and J. Bragg, J. Chem. Phys. **31**, 526 (1959).
[6] D. Poland and H. A. Scheraga, *Theory of Helix-Coil Transitions in Biopolymers* (Academic Press, New York, 1970).
[7] A. V. Badasyan, A. Giacometti, Y. Sh. Mamasakhlisov, V. F. Morozov, and A. S. Benight, Phys. Rev. E **81**, 021921 (2010).
[8] M. Bachmann, *Thermodynamics and Statistical Mechanics of Macromolecular Systems* (Cambridge University Press, Cambridge, 2014).
[9] J. P. Kemp and Z. Y. Chen, Phys. Rev. Lett. **81**, 3880 (1998).
[10] D. C. Rapaport, Phys. Rev. E **66**, 011906 (2002).
[11] V. Varshney and G. A. Carri, Phys. Rev. Lett. **95**, 168304 (2005).
[12] S. A. Sabeur, Central Eur. J. Phys. **12**, 421 (2014).
[13] S. R. Presnell and F. E. Cohen, Proc. Natl. Acad. Sci. U.S.A. **86**, 6592 (1989).
[14] Z. Guo, C. L. Brooks III, and E. M. Boczko, Proc. Natl. Acad. Sci. U.S.A. **94**, 10161 (1997).
[15] C. Zhang, J. Hou, and S. H. Kim, Proc. Natl. Acad. Sci. U.S.A. **99**, 3581 (2002).
[16] S. W. Bruun, V. Iešmantavičius, J. Danielsson, and F. M. Poulsen, Proc. Natl. Acad. Sci. U.S.A. **107**, 13306 (2010).
[17] T. Bereau, M. Bachmann, and M. Deserno, J. Am. Chem. Soc. **132**, 13129 (2010).
[18] T. Bereau, M. Deserno, and M. Bachmann, Biophys. J. **100**, 2764 (2011).
[19] P. Palenčár and T. Bleha, Comput. Theor. Chem. **1006**, 62 (2013).
[20] Z. Qin, A. Fabre, and M. J. Buehler, Eur. Phys. J. E **36**, 53 (2013).
[21] G. C. Rollins and K. A. Dill, J. Am. Chem. Soc. **136**, 11420 (2014).
[22] S. Schnabel, T. Vogel, M. Bachmann, and W. Janke, Chem. Phys. Lett. **476**, 201 (2009).
[23] S. Schnabel, M. Bachmann, and W. Janke, J. Chem. Phys. **131**, 124904 (2009).
[24] D. T. Seaton, S. Schnabel, D. P. Landau, and M. Bachmann, Phys. Rev. Lett. **110**, 028103 (2013).
[25] K. Kremer and G. S. Grest, J. Chem. Phys. **92**, 5057 (1990).
[26] R. H. Swendsen and J. S. Wang, Phys. Rev. Lett. **57**, 2607 (1986).
[27] K. Hukushima and K. Nemoto, J. Phys. Soc. Jpn. **65**, 1604 (1996).
[28] K. Hukushima, H. Takayama, and K. Nemoto, Int. J. Mod. Phys. C **07**, 337 (1996).
[29] C. J. Geyer, *Computing Science and Statistics: Proceedings of the 23rd Symposium on the Interface*, edited by E. M. Keramidas (Interface Foundation, Fairfax Station VA, 1991), 156.
[30] S. Schnabel, M. Bachmann, and W. Janke, Phys. Rev. Lett. **98**, 048103 (2007).
[31] C. Junghans, M. Bachmann, and W. Janke, Phys. Rev. Lett. **97**, 218103 (2006).
[32] C. Junghans, M. Bachmann, and W. Janke, J. Chem. Phys. **128**, 085103 (2008).
[33] M. J. Williams and M. Bachmann (to be published).